
mKG-RAG: Multimodal Knowledge Graph-Enhanced RAG for Visual Question Answering

Xu Yuan

Department of Computing
The Hong Kong Polytechnic University
Hong Kong SAR, China
xuyuan127@gmail.com

Liangbo Ning

Department of Computing
The Hong Kong Polytechnic University
Hong Kong SAR, China
BigLemon1123@gmail.com

Wenqi Fan *

Department of Computing
The Hong Kong Polytechnic University
Hong Kong SAR, China
wenqifan03@gmail.com

Qing Li *

Department of Computing
The Hong Kong Polytechnic University
Hong Kong SAR, China
qing-prof.li@polyu.edu.hk

Abstract

Recently, Retrieval-Augmented Generation (RAG) has been proposed to expand internal knowledge of Multimodal Large Language Models (MLLMs) by incorporating external knowledge databases into the generation process, which is widely used for **knowledge-based Visual Question Answering (VQA)** tasks. Despite impressive advancements, vanilla RAG-based VQA methods that rely on unstructured documents and overlook the structural relationships among knowledge elements frequently introduce irrelevant or misleading content, reducing answer accuracy and reliability. To overcome these challenges, a promising solution is to integrate **multimodal knowledge graphs (KGs)** into RAG-based VQA frameworks to enhance the generation by introducing structured multimodal knowledge. Therefore, in this paper, we propose a novel multimodal knowledge-augmented generation framework (**mKG-RAG**) based on multimodal KGs for knowledge-intensive VQA tasks. Specifically, our approach leverages MLLM-powered keyword extraction and vision-text matching to distill semantically consistent and modality-aligned entities/relationships from multimodal documents, constructing high-quality multimodal KGs as structured knowledge representations. In addition, a dual-stage retrieval strategy equipped with a question-aware multimodal retriever is introduced to improve retrieval efficiency while refining precision. Comprehensive experiments demonstrate that our approach significantly outperforms existing methods, setting a new state-of-the-art for knowledge-based VQA.

1 Introduction

Visual Question Answering (VQA) [2, 19] is a challenging task at the intersection of vision and language understanding, requiring models to interpret images and answer related questions. This capability has enabled remarkable advances in various domains, including medical image diagnosis [33] and customer service support [12]. Recently, due to the powerful visual-linguistic understanding and reasoning capabilities, Multimodal Large Language Models (**MLLMs**) [35, 30, 50, 7] have provided a promising solution to conventional VQA tasks. For instance, LLaVA [35] demonstrates strong

*Corresponding author

zero-shot performance on commonsense VQA by leveraging pre-trained visual encoders for image representation alongside the reasoning capabilities of large language models (LLMs). Despite notable advancements, MLLMs face critical limitations in knowledge-intensive VQA scenarios [40, 6] (termed **knowledge-based VQA**), particularly those requiring encyclopedic knowledge, long-tail factual recall, or contextual reasoning beyond immediate visual inputs. As illustrated in Figure 1 (a), when queried about the latest renovation date of a stadium, typical MLLMs exhibit two characteristic failure modes: generating plausible but factually incorrect responses or refusing to answer altogether. These issues stem from the scarcity of relevant knowledge in MLLMs’ training corpus and the inherent difficulty of memorizing low-frequency facts [6].

Recently, Retrieval-Augmented Generation (**RAG**) [16] has shown great potential in addressing these challenges by leveraging external knowledge databases to supplement the internal knowledge of MLLMs, thereby enabling more accurate answer generation [32, 4, 11]. Specifically, multiple query-relevant documents are retrieved from external knowledge databases and serve as in-context information to augment the generation process of MLLMs. Despite their success, vanilla RAG-based VQA methods that rely on unstructured documents or paragraphs often introduce irrelevant or even misleading information [38, 51], thereby compromising the accuracy and reliability of generated answers. Moreover, these approaches typically overlook the structural relationships among knowledge elements, limiting the reasoning capabilities of MLLMs. As illustrated in Figure 1 (b), the presence of noisy and unstructured context makes it difficult for MLLMs to identify and leverage relevant supporting evidence. To overcome these limitations, a promising direction is to retrieve structured knowledge, such as Knowledge Graphs (KGs) [23] for augmentation generation [22, 15, 59]. However, in the VQA setting, which inherently involves multimodal reasoning, relying solely on textual KGs is suboptimal, as both modalities are crucial for identifying relevant knowledge. Therefore, integrating **Multimodal Knowledge Graphs** into the retrieval-augmented VQA framework presents a more robust solution to generate reliable and precise responses in knowledge-intensive scenarios, as illustrated in Figure 1 (c).

However, retrieving relevant knowledge from multimodal knowledge graphs to enhance the generation of knowledge-based VQA tasks is exceptionally challenging. First, off-the-shelf multimodal KGs [36] are generally built around common entities, and often lack the encyclopedic or long-tail knowledge required by knowledge-intensive questions, rendering them ineffective for direct use in knowledge-based VQA. Moreover, current knowledge sources used in knowledge-based VQA [40, 6] are typically organized in unstructured documents containing substantial contextual noise, making it challenging to extract well-structured entities and relationships essential for constructing high-quality multimodal KGs. Furthermore, a large-scale knowledge graph constructed from millions of documents, each potentially containing hundreds of entities and relationships, significantly expands the search space. Consequently, performing direct retrieval over such a graph is computationally inefficient and adversely affects retrieval precision.

To address the challenges above, this paper proposes **mKG-RAG**, a novel

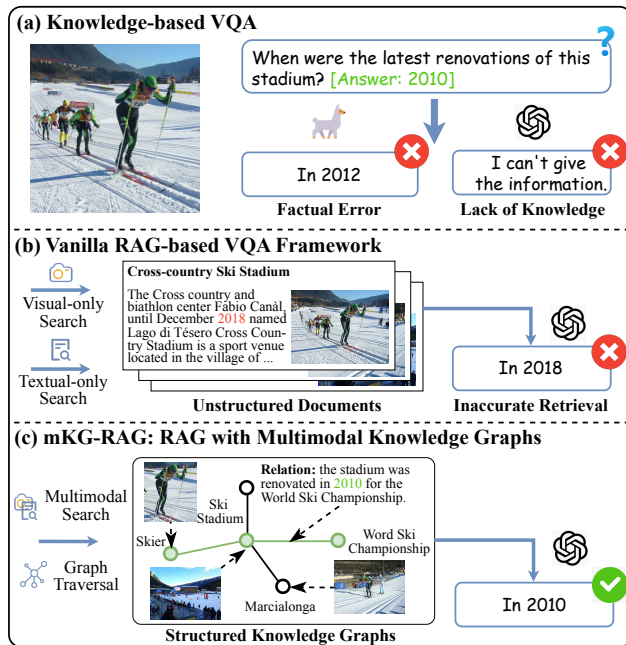


Figure 1: Illustration of issues in knowledge-based VQA. (b) Vanilla RA methods suffer from retrieving unstructured knowledge from external documents via unimodal retrievers. (c) Our mKG-RAG augments MLLMs with structural information from multimodal knowledge graphs.

retrieval-augmented generation framework integrated with multimodal knowledge graphs designed to enhance the reasoning capabilities of MLLMs in knowledge-based VQA tasks. More specifically, a multimodal knowledge graph construction module is introduced to transform unstructured multimodal documents, such as Wikipedia articles, into structured knowledge representations. This module leverages MLLM-powered keyword extraction and vision-text alignment to extract semantically consistent and modality-aligned entities and relationships from external multimodal documents. To enable efficient retrieval, mKG-RAG develops a dual-stage search paradigm that combines a coarse-grained document recall and a fine-grained entity/relationship retrieval. The coarse stage efficiently narrows the search space by identifying candidate documents likely to contain relevant evidence, while the fine stage refines the results by retrieving query-relevant entities and relationships from multimodal KGs that are dynamically constructed from these potentially noisy documents. During retrieval, unlike previous methods that rely on isolated unimodal retrievers, we introduce a question-aware multimodal retriever trained on a high-quality question-evidence dataset to further enhance retrieval precision within the proposed search paradigm. Comprehensive evaluations on two frequently used benchmarks demonstrate the superior performance of mKG-RAG, achieving an accuracy of 36.3% on E-VQA and 40.5% on InfoSeek.

The contributions of this work are summarized as follows:

- We propose mKG-RAG, a novel multimodal knowledge-augmented generation framework that integrates RAG with multimodal KGs to enhance the knowledge reasoning of MLLMs. To the best of our knowledge, this is the first work to investigate the potential of multimodal knowledge graphs in knowledge-intensive VQA tasks.
- Our framework develops a multimodal KG construction pipeline, allowing the extraction of image-text aligned entities and relations from multimodal documents. Additionally, a dual-stage retrieval schema with a question-aware multimodal retriever enables us to unleash the potential of RAG incorporated with multimodal KGs.
- Extensive experiments demonstrate that mKG-RAG significantly outperforms strong baselines, setting new state-of-the-art results on E-VQA and InfoSeek.

2 Related Work

Benefiting from the rapid advancement of Large Language Models [8, 49, 9, 57, 18, 17, 45, 42], Multimodal Large Language Models have shown prominent understanding and reasoning abilities across diverse vision-language tasks [35, 50, 55]. Beyond the LLM backbone, MLLMs incorporate two key components: a vision encoder and a vision-language integration module. The former typically uses a pre-trained visual encoder [14], while the latter varies significantly in design, like MLP-based projectors [35], Perceiver [1], and Q-Former [13]. While MLLMs excel at processing human queries and interpreting visual context, they remain prone to knowledge gaps and hallucinations. Although this issue is inherent to all LLMs, it is more pronounced in MLLMs due to the limited availability of high-quality, large-scale multimodal data.

While traditional VQA [2, 19] benchmarks evaluate vision-language understanding primarily within the visual context, knowledge-intensive VQA significantly increases the challenge by requiring specific or detailed knowledge beyond the image content. Early benchmarks such as OK-VQA [39] and A-OKVQA [48] highlight the importance of commonsense knowledge in VQA, which can be effectively addressed by MLLMs trained on large and diverse corpora. However, E-VQA [40] and InfoSeek [6] introduced greater challenges by encompassing a broad range of Wikipedia entities and requiring fine-grained knowledge about them. Consequently, modern MLLMs often fail to answer such questions accurately, as the relevant knowledge is either missing or represents long-tail distributions in their training data.

RAG is commonly used in LLMs to tackle issues such as outdated information and hallucinations [16, 41]. By dynamically combining external knowledge with the model’s built-in abilities, RAG offers an efficient approach for tasks requiring extensive knowledge. Inspired by this, RA-VQA [31], Wiki-LLaVA [4], and EchoSight [53] have successfully applied retrieval augmentation to knowledge-intensive VQA, but their retrieval suffers from the modality gap [29] between multimodal queries and textual knowledge bases. Recent studies [11, 56] leveraged MLLMs to identify relevant information from retrieved passages, which depend on multiple calls to MLLMs and lead to substantially higher inference overhead. Moreover, existing RAG-based methods typically retrieve

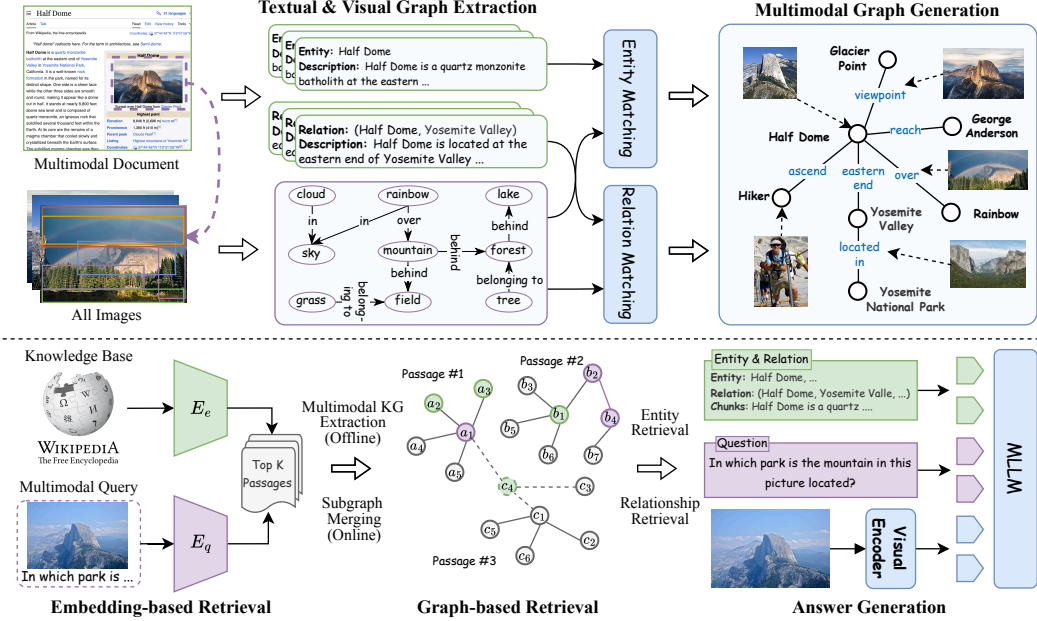


Figure 2: An overview of our mKG-RAG consists of a multimodal knowledge graph construction pipeline (top) and a dual-stage retrieval paradigm for answer generation (bottom).

unstructured documents, overlooking both the noise present in retrieval sources and the logical relationships among knowledge elements. This results in noisy and disorganized knowledge that increases the reasoning burden on MLLMs. To address this challenge, recent research has begun exploring the use of Knowledge Graphs (KGs), which provide structured representations of entities and their relationships, to enhance the generative capabilities of LLMs [22, 27, 15, 59, 38]. However, these efforts primarily focus on textual KGs, leaving the potential of multimodal KGs largely underexplored. To bridge this gap, our work is the first to integrate multimodal KGs into the RAG framework, specifically designed for vision-language tasks that require fine-grained external knowledge.

3 The Proposed Method: mKG-RAG

In the knowledge-based VQA task, the model receives an image-question pair (I_q, q) as input and is required to generate a textual answer a , potentially leveraging an accessible knowledge base \mathcal{B} as additional context. In our setting, the knowledge source is composed of multimodal documents featuring both text articles T and their corresponding image assets I , *i.e.*, $\mathcal{B} = \{(T_i, I_i)\}_{i=1}^N$. The core objectives of our multimodal retrieval-augmented generation framework are twofold: (1) to effectively convert the unstructured knowledge base \mathcal{B} into structured multimodal KGs, and (2) to precisely retrieve query-relevant knowledge from multimodal KGs while capturing the underlying structural relationships, thereby augmenting the knowledge scope of MLLMs.

The visual workflow of the proposed mKG-RAG is depicted in Figure 2, showcasing two key innovations. First, a multimodal knowledge graph construction pipeline is introduced, leveraging MLLMs to convert plain multimodal documents into structured knowledge representations, *i.e.*, graphs. Then, a dual-stage retrieval paradigm is proposed to perform fine-grained graph retrieval over a query-specific multimodal KG constructed from subgraphs of documents initially retrieved through coarse-grained vector search.

3.1 Multimodal Knowledge Graph Construction

Existing retrieval-augmented VQA models struggle with noisy context and overlook structural relationships due to retrieving fragmented textual chunks. A promising solution is to retrieve from structured knowledge sources, such as knowledge graphs. Nevertheless, the off-the-shelf multimodal KGs [36] are typically designed for common entities, which is unsuitable for addressing VQA cases involving detailed or long-tail knowledge, not to mention the domain-specific or even private

knowledge. Thus, this work explores an effective multimodal KG construction pipeline to extract semantic-consistent and modality-aligned entities and relationships from accessible multimodal documents for the task of knowledge-based VQA. Specifically, for each document $(T, I) \in \mathcal{B}$, where article $T = \{t_1, \dots, t_n\}$ typically contains multiple sections and $I = \{i_1, \dots, i_m\}$ is a set of images, we first segment it into manageable pieces. Sections without images are split or merged based on a fixed chunk size [16], while sections containing images are preserved in their entirety to maintain alignment between images and text. As illustrated in Figure 2, each segment is then processed by three key modules. Textual Graph Extraction identifies entities and their relationships from text, while Visual Graph Extraction detects prominent objects and their interactions from images. Finally, the Multimodal Graph Generation module fuses the textual and visual entities and relations into a unified multimodal graph.

Textual Graph Extraction. Following prior work [20], we process each textual piece by prompting LLMs to identify key entities (nodes) and meaningful relationships (edges), thereby forming a textual subgraph $\mathcal{G}_t = (\mathcal{N}, \mathcal{E})$. Like the example in Figure 2, each entity n_i in \mathcal{N} contains a unique name and a detailed description, offering an abstract representation to facilitate subsequent retrieval. Each relationship $e_{ij} \in \mathcal{E}$ connects head and tail entities (n_i, n_j) and includes a concise relation summary.

Visual Graph Extraction. The textual subgraph has distilled the skeleton of textual chunks, including informative entities and relationships, but it lacks visual elements, a critical component in VQA tasks. A naive strategy is to supply \mathcal{G}_t with corresponding images [36] directly. However, considering that images often contain multiple objects and background noise, we propose augmenting the textual subgraph with fine-grained region information. Each region possibly represents an individual entity or a relationship among two or more entities, as depicted in Figure 2. For simplicity, this work focuses exclusively on binary relationships, leaving the study of hyper-relationships [37] for future research.

Specifically, we employ the Scene Graph Generation (SGG) techniques [25] to extract a precise visual graph for each image in I . The visual graph is formalized as $\mathcal{G}_v = (\mathcal{V}, \mathcal{R})$, where $\mathcal{V} = \{v_i\}_{i=1}^{N_v}$ represents the set of visual objects with predicted category labels and bounding boxes, and $\mathcal{R} = \{r_{ij}\}_{i \neq j}$ denotes the visual relationships between objects. Unlike object detection [47], SGG offers additional relational information, facilitating efficient vision-text relationship matching.

Multimodal Graph Generation. At the core of the construction pipeline lies the challenge of merging the textual and visual graphs into a semantic-consistent and modality-aligned multimodal graph. Directly matching textual and visual entities/relationships based on image-text similarity [46] is limited to shallow or global alignment, lacking the capacity to capture fine-grained and contextual correspondences. Given the impressive vision-language understanding abilities of MLLMs [35], a promising solution is to employ MLLMs as the vision-text matcher, effectively aligning semantically consistent visual and textual entities/relationships. Thus, the following prompt is designed:

Vision-Text Matching Prompt: <Prefix Instruction> <IMAGE> [Textual Entities & Relationships]
[Visual Entities & Relationships]

Here, <Prefix Instruction> explains the input format of textual and visual graphs and guides the MLLMs in matching their entities and relationships. <IMAGE> denotes the corresponding image of the visual graph and contains only the original image, without extra regions. To enable MLLMs to comprehend graph structures, we convert both \mathcal{G}_t and \mathcal{G}_v into natural language format. For \mathcal{G}_t , each entity and relationship is expressed using its name and associated description, formatted as a sentence. The visual objects and relationships in \mathcal{G}_v are encoded as “<Object-ID>: <category>, <bbox>” and “<Relation-ID>: <subject>, <relation>, <object>”, respectively. Importantly, visual entities include only the predicted category and normalized bounding box, from which MLLMs can locate the corresponding region within <IMAGE>, without requiring actual regional images [54]. This design enables efficient inference by allowing simultaneous processing of all objects and relations in \mathcal{G}_v . To ensure MLLMs follow the prefix instruction and produce the desired output, we further enhance their reasoning ability by providing several high-quality exemplars. Detailed prompts are provided in Appendix A.

The whole process of vision-text matching is denoted as:

$$\mathcal{M} = \{(n, v)_i\}_{i=1}^{N_e} \cup \{(e, r)_j\}_{j=1}^{N_r} = \mathcal{F}_{mllm}(I, \mathcal{G}_t, \mathcal{G}_v). \quad (1)$$

Here, \mathcal{M} denotes a set comprising N_e matched entities and N_r matched relationships. As depicted in Figure 2, the image region of v (r) is attached as an attribute to its corresponding textual counterpart

n (e). Since a visual relationship r involves two object regions, we merge them using the union of their bounding boxes.

Through the above steps, we generate an image-text-aligned multimodal subgraph \mathcal{G} for each document segment. These subgraphs are then aggregated into a complete graph by merging identical nodes and edges. Notably, only subgraphs from the same document are merged, ensuring that each document produces an independent multimodal KG. During retrieval, relevant KGs from different documents are dynamically composed based on the retrieval results. Since the construction process is query-independent, the entire pipeline can be executed offline, and each document requires processing only once.

3.2 Dual-stage Retrieval Paradigm

To unleash the potential of constructed multimodal KGs, we further introduce a dual-stage retrieval framework inspired by human cognitive processes. When encountering unfamiliar multimodal queries, humans typically: (1) filter relevant supporting evidence from vast external multimodal sources, then (2) analyze and organize the extracted information into coherent structures for reasoning [59]. Our framework accordingly implements a coarse-grained vector similarity search followed by fine-grained graph retrieval.

Embedding-based Retrieval. For large-scale knowledge bases containing millions of passages, direct graph retrieval is inefficient, as each passage may include hundreds of nodes and edges, greatly expanding the search space. Thus, we first perform coarse-grained recall using vector search to identify candidates. Given a query (I_q, q) and a set of multimodal articles $\{(T_i, I_i)\}_{i=1}^N$, a similarity matrix \mathbf{S} can be obtained:

$$\mathbf{S} = \{s_i = \langle \mathcal{E}_q(I_q, q) \cdot \mathcal{E}_e(I_i, T_i) \rangle, i = 1, \dots, N\}, \quad (2)$$

where $\langle \cdot \rangle$ denotes the cosine similarity; \mathcal{E}_q and \mathcal{E}_e are multimodal encoders designed for query and evidence, respectively, as shown in Figure 3. Based on matrix \mathbf{S} , the top K_d highest-scoring documents are collected.

Graph-based Retrieval. Previous methods retrieve text chunks directly from candidate documents [53], which often introduces contextual noise and impairs reasoning performance. In contrast, our approach performs graph-based retrieval to identify query-relevant entities and relationships. These entities and relationships serve as distilled knowledge representations, significantly reducing noise and enabling more accurate retrieval.

Specifically, a query-specific multimodal graph \mathcal{G}_m is constructed by merging the offline-generated subgraphs corresponding to the candidate documents retrieved in the first stage. By limiting the merge to only relevant documents, such an online strategy effectively reduces ambiguous entities and relationships that often arise from cross-document knowledge inconsistencies [15]. Next, query-relevant entities and relationships are identified by computing embedding similarities between the multimodal query and each entity/relationship in \mathcal{G}_m . The embedding vector of the given entity and relationship can be formalized as $f_e = \mathcal{E}_e(n, v)$ and $f_r = \mathcal{E}_e(e, r)$. Here, top K_g best-matched candidates will be selected, *e.g.*, the entity a_1 and the relationship (b_2, b_4) in Figure 2. Combining K_g matched entities or relationships, we get a relevant subgraph \mathcal{G}_r^0 . However, similarity-based retrieval alone may yield incomplete information, potentially omitting critical evidence to answer the question entirely. To this end, we leverage the inherent structural properties of the graph and expand \mathcal{G}_r by incorporating information from its l -hop neighbors, *i.e.*,

$$\mathcal{G}_r^l = \text{Graph Traversal}(\mathcal{G}_m, \mathcal{G}_r^0, l), \quad (3)$$

where Graph Traversal is implemented by the breadth-first search. Notably, we selectively incorporate only query-relevant neighbors, as shown by the green nodes in Figure 2.

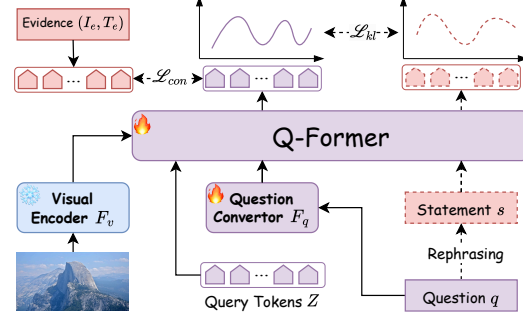


Figure 3: Architecture Design of Question-aware Multimodal Retriever.

Table 1: Retrieval performance on E-VQA set

| Model | Ret. Mode | E-VQA | | | | |
|---------------|-----------|-------------|-------------|-------------|-------------|-------------|
| | | R@1 | R@5 | R@10 | R@20 | R@50 |
| Nomic-text | T→T | 2.0 | 4.1 | 5.6 | 7.8 | 11.1 |
| Nomic-vision | V→V | 9.3 | 23.0 | 29.3 | 36.0 | 45.6 |
| CLIP ViT-L/14 | T→T | 2.0 | 4.7 | 6.4 | 8.8 | 12.1 |
| CLIP ViT-L/14 | V→V | 11.2 | 28.5 | 36.2 | 44.1 | 54.8 |
| CLIP ViT-L/14 | T→V | 1.1 | 3.1 | 4.6 | 7.3 | 12.3 |
| CLIP ViT-L/14 | V→T | 3.8 | 10.2 | 13.6 | 18.0 | 23.9 |
| QM-Retriever | MM | 18.9 | 36.8 | 46.2 | 55.6 | 66.7 |

Table 2: Retrieval performance on InfoSeek set

| Model | Ret. Mode | InfoSeek | | | | |
|---------------|-----------|-------------|-------------|-------------|-------------|-------------|
| | | R@1 | R@5 | R@10 | R@20 | R@50 |
| Nomic-text | T→T | 11.0 | 19.3 | 24.2 | 30.4 | 40.6 |
| Nomic-vision | V→V | 35.0 | 56.5 | 63.3 | 69.3 | 75.5 |
| CLIP ViT-L/14 | T→T | 9.2 | 15.8 | 19.3 | 23.3 | 30.0 |
| CLIP ViT-L/14 | V→V | 40.0 | 63.4 | 70.9 | 77.7 | 83.7 |
| CLIP ViT-L/14 | T→V | 8.5 | 18.8 | 24.6 | 31.7 | 42.5 |
| CLIP ViT-L/14 | V→T | 20.1 | 40.1 | 49.2 | 58.3 | 68.9 |
| QM-Retriever | MM | 49.7 | 71.6 | 78.0 | 82.5 | 89.1 |

The retrieved context comprises both graph elements (entities and relationships) and their associated textual segments. The former provides a structured knowledge outline, while the latter supplies the contextual details. Finally, the concatenated image, question, and context are fed into MLLMs for answer generation.

Question-aware Multimodal Retriever. Standard multimodal retrievers are optimized for semantic similarity rather than question relevance, often failing to retrieve precise evidence needed for answer generation, even if the returned content is semantically related. To address this issue, this work proposes a Question-aware Multimodal Retriever (QM-Retriever) targeting evidence retrieval for VQA tasks.

As shown in Figure 3, the retriever is adapted from the Q-Former [28] by incorporating an additional Visual Encoder \mathcal{F}_v and a Question Converter \mathcal{F}_q . We employ the BLIP-2 [28] pre-trained vision encoder as \mathcal{F}_v to extract image features. The Question Converter reformulates interrogative questions into declarative forms to address grammatical mismatches with evidence texts, which could otherwise hinder retrieval accuracy. Importantly, the reformulation process occurs in the latent space rather than the language space. Given an image-question pair (I_q, q) , QM-Retriever encodes it into a fix-sized embedding Z_q :

$$Z_q = \text{Q-Former}(Z, \mathcal{F}_v(I_q), \mathcal{F}_q(q)), \quad (4)$$

where Z is a set of learnable tokens introduced by Q-Former. The resulting embedding Z_q can then be used for vector-based retrieval. Note that the QM-Retriever omits the Question Converter when operating as the evidence encoder.

To optimize the QM-Retriever, a query-evidence dataset is built based on the training set of E-VQA [40], where each multimodal query (I_q, q) is paired with its corresponding ground-truth evidence (I_e, T_e) . Here, T_e represents evidence text, and I_e refers to the associated image from the evidence section. For sections without visual content, black images are used as placeholders.

The optimization of our QM-Retriever involves two key objectives: (1) *Question-Evidence Alignment*. To retrieve query-relevant evidence, we employ contrastive learning [21, 5] to align the features of multimodal query and evidence by encouraging positive query-evidence pairs to have similar representations in contrast to the negative pairs in a batch, *i.e.*,

$$\mathcal{L}_{con} = -\log \frac{\exp(\text{sim}(Z_q, Z_e)/\tau)}{\sum_{k=1}^B \exp(\text{sim}(Z_q, Z_k)/\tau)}. \quad (5)$$

Here, B denotes the batch size, and τ is a temperature parameter. (2) *Question Reformulation*. We leverage LLMs to convert the original question q into a declarative statement s that emphasizes the scene context. By encoding (I_q, s) with QM-Retriever, we obtain a declarative representation Z_s as a reference. Then, Kullback-Leibler divergence is measured to minimize the divergence between the distributions of Z_q and Z_s . Finally, the total objective is formulated as the linear combination controlled by a hyperparameter:

$$\mathcal{L} = \mathcal{L}_{con} + \alpha D_{KL}(p(Z_q|I_q, q) \parallel p((Z_s|I_q, s))). \quad (6)$$

Notably, the Q-Former is initialized with BLIP-2’s weights and fine-tuned jointly with \mathcal{F}_q , while \mathcal{F}_v remains frozen.

Table 3: Main results of models with external knowledge on the E-VQA and InfoSeek datasets. ^{*} denotes that the model is further fine-tuned on the corresponding dataset. [†] and [‡] represent the variant of our mKG-RAG with different retrievers.

| Model | LLM / MLLM | Retrieval Mode | | | E-VQA | | InfoSeek | | |
|---|--------------|----------------|------|-------|-------------|-------------|-------------|-------------|-------------|
| | | Retriever | Text | Image | Single-Hop | All | Unseen-Q | Unseen-E | All |
| <i>Zero-shot MLLMs</i> | | | | | | | | | |
| BLIP-2 [28] | Flan-T5XL | – | ✗ | ✗ | 12.6 | 12.4 | 12.7 | 12.3 | 12.5 |
| InstructBLIP [13] | Flan-T5XL | – | ✗ | ✗ | 11.9 | 12.0 | 8.9 | 7.4 | 8.1 |
| LLaVA-v1.5 [34] | Vicuna-7B | – | ✗ | ✗ | 16.3 | 16.9 | 9.6 | 9.4 | 9.5 |
| LLaVA-More [10] | LLaMA-3.1-8B | – | ✗ | ✗ | 15.8 | 16.0 | 9.0 | 8.2 | 8.6 |
| Qwen2-VL [50] | Qwen2-VL-7B | – | ✗ | ✗ | 19.9 | 19.7 | 19.8 | 18.5 | 19.2 |
| <i>Retrieval-Augmented Models</i> | | | | | | | | | |
| RORA-VLM [44] | Vicuna-7B | CLIP + GS | ✓ | ✓ | – | 20.3 | 25.1 | 27.3 | – |
| Wiki-LLaVA [*] [4] | Vicuna-7B | CLIP ViT-L/14 | ✓ | ✗ | 21.8 | 26.4 | 30.1 | 27.8 | 28.9 |
| EchoSight [53] | LLaMA-3.1-8B | EVA-CLIP-8B | ✓ | ✗ | 22.4 | 21.7 | 30.0 | 30.7 | 30.4 |
| EchoSight [53] | LLaMA-3.1-8B | EVA-CLIP-8B | ✗ | ✓ | 26.4 | 24.9 | 18.0 | 19.8 | 18.8 |
| mR2AG [*] [56] | Vicuna-7B | CLIP ViT-L/14 | ✗ | ✓ | – | – | 40.6 | 39.8 | 40.2 |
| ReflectiVA [*] [11] | LLaMA-3.1-8B | EVA-CLIP-8B | ✓ | ✗ | 28.0 | 29.2 | 40.4 | 39.8 | 40.1 |
| ReflectiVA [*] [11] | LLaMA-3.1-8B | EVA-CLIP-8B | ✗ | ✓ | 35.5 | 35.5 | 28.6 | 28.1 | 28.3 |
| <i>Graph Retrieval-Augmented Models</i> | | | | | | | | | |
| mKG-RAG [†] | LLaMA-3.1-8B | CLIP ViT-L/14 | ✓ | ✗ | 24.4 | 23.4 | 24.1 | 22.3 | 23.2 |
| mKG-RAG [‡] | LLaMA-3.1-8B | CLIP ViT-L/14 | ✗ | ✓ | 24.6 | 23.7 | 21.3 | 19.8 | 20.6 |
| mKG-RAG | LLaMA-3.1-8B | QM-Retriever | ✓ | ✓ | 27.1 | 26.1 | 32.9 | 31.3 | 32.1 |
| mKG-RAG ^{*†} | LLaMA-3.1-8B | CLIP ViT-L/14 | ✓ | ✗ | 36.6 | 34.9 | 29.8 | 28.5 | 29.1 |
| mKG-RAG ^{*‡} | LLaMA-3.1-8B | CLIP ViT-L/14 | ✗ | ✓ | 32.9 | 31.0 | 29.4 | 27.3 | 28.3 |
| mKG-RAG [*] | LLaMA-3.1-8B | QM-Retriever | ✓ | ✓ | 38.4 | 36.3 | 41.4 | 39.6 | 40.5 |

4 Experiments

4.1 Experimental Setup

Datasets and Knowledge Base. Our method is evaluated on **E-VQA** [40] and **InfoSeek** [6], which contain question-answer pairs linked to documents from Wikipedia. E-VQA offers a knowledge base comprising 2M Wikipedia pages, where each question-answer pair is annotated with supporting Wikipedia articles, relevant evidence paragraphs, and associated images. For InfoSeek, since there is no publicly released knowledge base, we utilize a subset of 100K documents from E-VQA filtered by EchoSight [53] as our knowledge source.

Implementation Details. We use the Llama-3.2-11B-Vision model as the MLLM for multimodal KG Construction, including textual entity-relationship recognition and vision-text matching. A lightweight one-stage SGG model, EGTR [25], is applied to produce scene graphs for images in the knowledge base. In the first-stage retrieval, we utilize the FAISS [26] for efficient approximate nearest neighbor search and select the top 10 (K_d) best-matched documents. For the graph retrieval, we empirically set the K_g and l to 10 and 1, respectively. Unless otherwise indicated, we adopt LLaVA-More [10] as the multimodal answer generator, following the setup in ReflectiVA [11]. More details are provided in the *Appendix.B*.

4.2 Performance Comparison

Results on Retrieval. To assess the effectiveness of multimodal retrieval using QM-Retriever, we conduct comparative analyses against unimodal and cross-modal retrievers in selecting the most relevant documents for VQA queries. Specifically, we use Nomic-Embed-v1.5 [43] and CLIP ViT-L/14@336 [46] as retrieval baselines and examine four feasible retrieval combinations: text-to-text ($T \rightarrow T$), vision-to-vision ($V \rightarrow V$), text-to-vision ($T \rightarrow V$), and vision-to-text ($V \rightarrow T$).

Table 1 and Table 2 report the Recall scores on E-VQA and InfoSeek, respectively. QM-Retriever consistently outperforms all baseline methods, achieving average improvements of 9.9% (E-VQA) and 7.0% (InfoSeek) over the second-best approach. The strong recall performance ensures that mKG-RAG operates on highly relevant knowledge graphs constructed in the fine-grained retrieval phase, as further supported by our ablation studies. Additionally, the results reveal that $V \rightarrow V$ retrieval consistently beats other unimodal and cross-modal configurations, underscoring the critical role of visual content in VQA tasks.

Table 4: VQA accuracy on E-VQA across different MLLM architectures with varying sizes

| MLLM | E-VQA | InternVL3 | LLaMA-3.2 | LLaVA-v1.5 | DeepSeek-VL2 | Qwen2.5-VL | | | | |
|-----------|------------|------------------|------------------|-----------------|------------------|-----------------|-----------------|-----------------|-----------------|-----------------|
| | | 8B | 11B | 7B | 13B | 3B | 16B | 3B | 7B | 32B |
| Zero-shot | Single-Hop | 22.4 | 27.0 | 15.8 | 16.1 | 22.0 | 22.4 | 19.1 | 21.0 | 27.1 |
| | All | 23.0 | 28.9 | 16.2 | 16.6 | 21.6 | 22.3 | 18.9 | 20.8 | 27.3 |
| mKG-RAG | Single-Hop | 32.7 | 37.2 | 25.0 | 27.7 | 28.4 | 31.1 | 28.9 | 30.4 | 36.5 |
| | All | 32.7 | 38.5 | 24.6 | 27.8 | 27.4 | 29.9 | 28.2 | 29.6 | 36.5 |
| | | ^{↑10.3} | ^{↑10.2} | ^{↑9.2} | ^{↑11.6} | ^{↑6.4} | ^{↑8.7} | ^{↑9.8} | ^{↑9.4} | ^{↑9.4} |
| | | ^{↑9.7} | ^{↑9.6} | ^{↑8.4} | ^{↑11.2} | ^{↑5.8} | ^{↑7.6} | ^{↑9.3} | ^{↑8.8} | ^{↑9.2} |

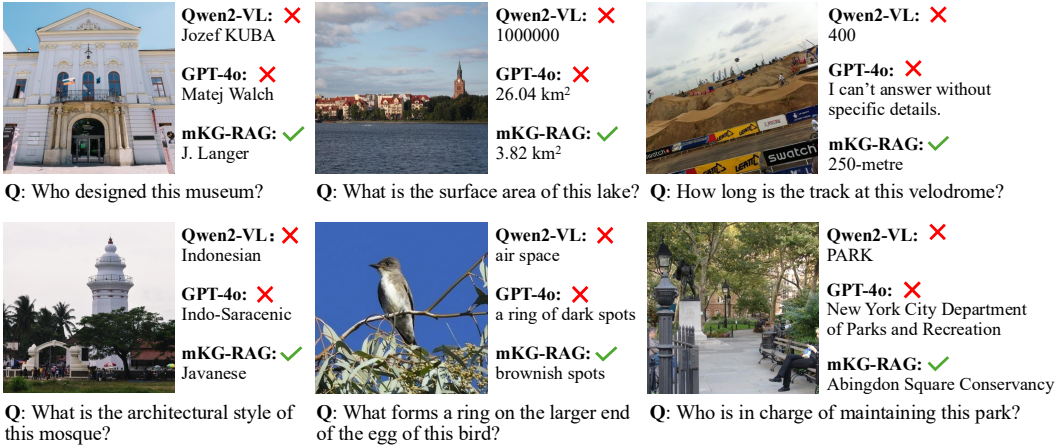


Figure 4: Qualitative results of Qwen2-VL-7B, GPT-4o and mKG-RAG on E-VQA dataset.

Results on E-VQA and InfoSeek. In this section, we compare mKG-RAG with Zero-shot MLLMs and RAG-based approaches on the benchmarks mentioned above. The results in Table 3 demonstrate that zero-shot MLLMs struggle with knowledge-based VQA tasks, particularly on the InfoSeek dataset. These limitations underscore the critical need for external knowledge integration. By augmenting LLaVA-More with mKG-RAG, we achieve substantial improvements, over 20.3% on E-VQA and 31.9% on InfoSeek, highlighting the value of retrieval augmentation.

Furthermore, our method achieves state-of-the-art performance on both datasets. Under the fine-tuning setting, mKG-RAG* surpasses both mR2AG* and ReflectiVA*. Even without fine-tuning, mKG-RAG outperforms EchoSight by 1.2% and 1.7%, respectively. These results highlight the advantages of integrating RAG with multimodal KGs and demonstrate the effectiveness of our QM-Retriever. Table 3 also includes two mKG-RAG variants that replace QM-Retriever with text-only and vision-only CLIP for entity/relationship retrieval, while still using documents retrieved by QM-Retriever to construct multimodal KGs. In the text-only variant, both questions and image captions are used as queries to provide more context, explaining its better performance over the vision-only version. However, they both remain less effective than our full approach with QM-Retriever.

Consistency across Architectures. In Table 4, we provide a detailed comparison of VQA scores across MLLMs of varying parameter sizes, including InternVL3 [58], LLaMA-3.2-Vision², LLaVA-v1.5 [34], DeepSeek-VL2 [52], and Qwen2.5-VL [3]. When enhanced with our mKG-RAG framework, these models achieve average performance gains of 9.4% on single-hop queries and 8.7% on overall scenarios, demonstrating the method’s strong generalization across different architectures and scales.

Qualitative Results. Figure 4 shows a qualitative comparison of mKG-RAG with zero-shot Qwen2-VL and GPT-4o. While the latter two tend to produce plausible but incorrect or evasive responses, mKG-RAG consistently handles knowledge-intensive queries, especially those involving precise numerical and temporal reasoning.

²<https://huggingface.co/meta-llama/Llama-3.2-11B-Vision>

Table 5: The ablation study of the design of mKG-RAG

| Method | E-VQA | | InfoSeek | | |
|---------------------|-------------|-------------|-------------|-------------|-------------|
| | Single-Hop | All | Un-Q | Un-E | All |
| mKG-RAG | 38.4 | 36.3 | 41.4 | 39.6 | 40.5 |
| w/o QM-Retriever | 34.2 | 31.6 | 38.9 | 37.9 | 38.4 |
| w/o Graph Retrieval | 30.1 | 28.2 | 33.3 | 32.7 | 33.0 |
| w/o Graph Expansion | 37.2 | 35.0 | 40.8 | 39.4 | 40.1 |

Table 6: The ablation study of how the retrieval number of entities/relationships affects the VQA accuracy on E-VQA.

| Model | Ret. Mode | $K_g = 1$ | $K_g = 5$ | $K_g = 10$ | $K_g = 20$ |
|--------------------|------------|-------------|-------------|-------------|-------------|
| mKG-RAG \dagger | Textual | 29.1 | 33.9 | 34.9 | 35.9 |
| mKG-RAG \ddagger | Visual | 23.0 | 29.6 | 31.0 | 32.0 |
| mKG-RAG | Multimodal | 29.2 | 35.1 | 36.3 | 36.9 |

4.3 Ablation Study

Impact of Coarse-grained Retrieval. To quantify the impact of coarse-grained document retrieval, we conduct an ablation experiment replacing QM-Retriever with visual-only CLIP (ViT-L/14@336) for top- K_d document selection. The results in Table 5 reveal significant performance drops: overall VQA accuracy of mKG-RAG decreases by 4.7% on E-VQA and 2.1% on InfoSeek. This ablation conclusively demonstrates the critical role of first-stage retrieval and QM-Retriever’s superiority over unimodal alternatives.

Effectiveness of Graph-based Retrieval. In our method, the entities and relationships extracted from documents form a distilled knowledge graph, reducing noise and enabling more effective retrieval than direct text chunk matching. To validate this insight, we replace graph-based retrieval with a naive chunk-based alternative. Specifically, we segment retrieved documents into fixed-size chunks and select those relevant to the given question and image description. As shown in Table 5, chunk-based retrieval leads to a substantial accuracy drop, 8.1% on E-VQA and 7.5% on InfoSeek.

Contribution of Graph Expansion. mKG-RAG enhances the constructed subgraph through l -hop neighbor expansion, effectively capturing potentially missing but relevant knowledge connections. Table 5 shows that omitting graph expansion leads to consistent performance drops of 1.3% (E-VQA) and 0.4% (InfoSeek), demonstrating its critical contribution to our mKG-RAG.

Impact of Varying Retrieval Number. In Table 6, we further analyze the impact of K_g , the number of retrieved entities and relationships, on our method. As K_g increases from 1 to 20, the overall accuracy of mKG-RAG and its variants gradually improves, as higher recall rates enhance the likelihood of capturing relevant knowledge. However, when $K_g > 10$, the benefit diminishes due to longer contexts and more noise. Thus, setting $K_g = 10$ offers a practical trade-off. Notably, mKG-RAG still performs competitively even at $K_g = 1$, thanks to its graph expansion strategy, which enables the model to gather additional relevant information.

5 Conclusion

We propose mKG-RAG, a novel retrieval-augmented generation framework that integrates multimodal knowledge graphs (KGs) to overcome the knowledge limitations of multimodal large language models (MLLMs). Our framework constructs structured, modality-aligned KGs using MLLM-driven keyword extraction and cross-modal alignment, and employs a dual-stage retrieval system, which combines vector-based and graph-based retrieval for precise knowledge augmentation. Extensive experiments show that mKG-RAG outperforms state-of-the-art methods, with ablation studies validating each component’s contributions.

References

- [1] *Alayrac Jean-Baptiste, Donahue Jeff, Luc Pauline, Miech Antoine, Barr Iain, Hasson Yana, Lenc Karel, Mensch Arthur, Millican Katherine, Reynolds Malcolm, others* . Flamingo: a visual language model for few-shot learning // Advances in neural information processing systems. 2022. 35. 23716–23736.
- [2] *Antol Stanislaw, Agrawal Aishwarya, Lu Jiasen, Mitchell Margaret, Batra Dhruv, Zitnick C Lawrence, Parikh Devi*. Vqa: Visual question answering // Proceedings of the IEEE international conference on computer vision. 2015. 2425–2433.
- [3] *Bai Shuai, Chen Keqin, Liu Xuejing, Wang Jialin, Ge Wenbin, Song Sibo, Dang Kai, Wang Peng, Wang Shijie, Tang Jun, Zhong Humen, Zhu Yuanzhi, Yang Mingkun, Li Zhaohai, Wan Jianqiang, Wang Pengfei, Ding Wei, Fu Zheren, Xu Yiheng, Ye Jiabo, Zhang Xi, Xie Tianbao, Cheng Zesen, Zhang Hang, Yang Zhibo, Xu Haiyang, Lin Junyang*. Qwen2.5-VL Technical Report. 2025.
- [4] *Caffagni Davide, Cocchi Federico, Moratelli Nicholas, Sarto Sara, Cornia Marcella, Baraldi Lorenzo, Cucchiara Rita*. Wiki-llava: Hierarchical retrieval-augmented generation for multimodal llms // Proceedings of the IEEE/CVF Conference on Computer Vision and Pattern Recognition. 2024. 1818–1826.
- [5] *Chen Ting, Kornblith Simon, Norouzi Mohammad, Hinton Geoffrey*. A simple framework for contrastive learning of visual representations // International conference on machine learning. 2020. 1597–1607.
- [6] *Chen Yang, Hu Hexiang, Luan Yi, Sun Haitian, Changpinyo Soravit, Ritter Alan, Chang Ming-Wei*. Can Pre-trained Vision and Language Models Answer Visual Information-Seeking Questions? // Proceedings of the 2023 Conference on Empirical Methods in Natural Language Processing. 2023. 14948–14968.
- [7] *Chen Zhe, Wu Jiannan, Wang Wenhui, Su Weijie, Chen Guo, Xing Sen, Zhong Muyan, Zhang Qinglong, Zhu Xizhou, Lu Lewei, others* . Internvl: Scaling up vision foundation models and aligning for generic visual-linguistic tasks // Proceedings of the IEEE/CVF conference on computer vision and pattern recognition. 2024. 24185–24198.
- [8] *Chiang Wei-Lin, Li Zhuohan, Lin Ziqing, Sheng Ying, Wu Zhanghao, Zhang Hao, Zheng Lianmin, Zhuang Siyuan, Zhuang Yonghao, Gonzalez Joseph E, others* . Vicuna: An open-source chatbot impressing gpt-4 with 90%* chatgpt quality // See <https://vicuna.lmsys.org> (accessed 14 April 2023). 2023. 2, 3, 6.
- [9] *Chung Hyung Won, Hou Le, Longpre Shayne, Zoph Barret, Tay Yi, Fedus William, Li Yunxuan, Wang Xuezhi, Dehghani Mostafa, Brahma Siddhartha, others* . Scaling instruction-finetuned language models // Journal of Machine Learning Research. 2024. 25, 70. 1–53.
- [10] *Cocchi Federico, Moratelli Nicholas, Caffagni Davide, Sarto Sara, Baraldi Lorenzo, Cornia Marcella, Cucchiara Rita*. LLaVA-MORE: A Comparative Study of LLMs and Visual Backbones for Enhanced Visual Instruction Tuning // arXiv preprint arXiv:2503.15621. 2025.
- [11] *Cocchi Federico, Moratelli Nicholas, Cornia Marcella, Baraldi Lorenzo, Cucchiara Rita*. Augmenting Multimodal LLMs with Self-Reflective Tokens for Knowledge-based Visual Question Answering // Proceedings of the IEEE/CVF Conference on Computer Vision and Pattern Recognition. 2025.
- [12] *Cui Can, Ma Yunsheng, Cao Xu, Ye Wengqian, Zhou Yang, Liang Kaizhao, Chen Jintai, Lu Juanwu, Yang Zichong, Liao Kuei-Da, others* . A survey on multimodal large language models for autonomous driving // Proceedings of the IEEE/CVF winter conference on applications of computer vision. 2024. 958–979.
- [13] *Dai Wenliang, Li Junnan, Li Dongxu, Tiong Anthony, Zhao Junqi, Wang Weisheng, Li Boyang, Fung Pascale, Hoi Steven*. InstructBLIP: Towards General-purpose Vision-Language Models with Instruction Tuning // Thirty-seventh Conference on Neural Information Processing Systems. 2023.

[14] *Dosovitskiy Alexey, Beyer Lucas, Kolesnikov Alexander, Weissenborn Dirk, Zhai Xiaohua, Unterthiner Thomas, Dehghani Mostafa, Minderer Matthias, Heigold Georg, Gelly Sylvain, Uszkoreit Jakob, Houlsby Neil.* An Image is Worth 16x16 Words: Transformers for Image Recognition at Scale // International Conference on Learning Representations. 2021.

[15] *Edge Darren, Trinh Ha, Cheng Newman, Bradley Joshua, Chao Alex, Mody Apurva, Truitt Steven, Metropolitansky Dasha, Ness Robert Osazuwa, Larson Jonathan.* From local to global: A graph rag approach to query-focused summarization // arXiv preprint arXiv:2404.16130. 2024.

[16] *Fan Wenqi, Ding Yujuan, Ning Liangbo, Wang Shijie, Li Hengyun, Yin Dawei, Chua Tat-Seng, Li Qing.* A survey on rag meeting llms: Towards retrieval-augmented large language models // Proceedings of the 30th ACM SIGKDD Conference on Knowledge Discovery and Data Mining. 2024. 6491–6501.

[17] *Fan Wenqi, Wang Shijie, Huang Jiani, Chen Zhikai, Song Yu, Tang Wenzhuo, Mao Haitao, Liu Hui, Liu Xiaorui, Yin Dawei, others .* Graph machine learning in the era of large language models (llms) // arXiv preprint arXiv:2404.14928. 2024.

[18] *Fan Wenqi, Zhou Yi, Wang Shijie, Yan Yuyao, Liu Hui, Zhao Qian, Song Le, Li Qing.* Computational Protein Science in the Era of Large Language Models (LLMs) // arXiv preprint arXiv:2501.10282. 2025.

[19] *Goyal Yash, Khot Tejas, Summers-Stay Douglas, Batra Dhruv, Parikh Devi.* Making the v in vqa matter: Elevating the role of image understanding in visual question answering // Proceedings of the IEEE conference on computer vision and pattern recognition. 2017. 6904–6913.

[20] *Guo Zirui, Xia Lianghao, Yu Yanhua, Ao Tu, Huang Chao.* LightRAG: Simple and Fast Retrieval-Augmented Generation // arXiv preprint arXiv:2410.05779. 2024.

[21] *He Kaiming, Fan Haoqi, Wu Yuxin, Xie Saining, Girshick Ross.* Momentum contrast for unsupervised visual representation learning // Proceedings of the IEEE/CVF conference on computer vision and pattern recognition. 2020. 9729–9738.

[22] *He Xiaoxin, Tian Yijun, Sun Yifei, Chawla Nitesh, Laurent Thomas, LeCun Yann, Bresson Xavier, Hooi Bryan.* G-retriever: Retrieval-augmented generation for textual graph understanding and question answering // Advances in Neural Information Processing Systems. 37. 2024. 132876–132907.

[23] *Hogan Aidan, Blomqvist Eva, Cochez Michael, d'Amato Claudia, Melo Gerard De, Gutierrez Claudio, Kirrane Sabrina, Gayo José Emilio Labra, Navigli Roberto, Neumaier Sebastian, others .* Knowledge graphs // ACM Computing Surveys (Csur). 2021. 54, 4. 1–37.

[24] *Hu Edward J, Shen Yelong, Wallis Phillip, Allen-Zhu Zeyuan, Li Yuanzhi, Wang Shean, Wang Lu, Chen Weizhu, others .* Lora: Low-rank adaptation of large language models. // ICLR. 2022. 1, 2, 3.

[25] *Im Jinbae, Nam JeongYeon, Park Nokyung, Lee Hyungmin, Park Seunghyun.* Egtr: Extracting graph from transformer for scene graph generation // Proceedings of the IEEE/CVF Conference on Computer Vision and Pattern Recognition. 2024. 24229–24238.

[26] *Johnson Jeff, Douze Matthijs, Jégou Hervé.* Billion-scale similarity search with GPUs // IEEE Transactions on Big Data. 2019. 7, 3. 535–547.

[27] *LUO LINHAO, Li Yuan-Fang, Haffari Gholamreza, Pan Shirui.* Reasoning on Graphs: Faithful and Interpretable Large Language Model Reasoning // The Twelfth International Conference on Learning Representations. 2024.

[28] *Li Junnan, Li Dongxu, Savarese Silvio, Hoi Steven.* Blip-2: Bootstrapping language-image pre-training with frozen image encoders and large language models // International conference on machine learning. 2023. 19730–19742.

[29] *Liang Victor Weixin, Zhang Yuhui, Kwon Yongchan, Yeung Serena, Zou James Y.* Mind the gap: Understanding the modality gap in multi-modal contrastive representation learning // Advances in Neural Information Processing Systems. 2022. 35. 17612–17625.

[30] *Lin Ji, Yin Hongxu, Ping Wei, Molchanov Pavlo, Shoeybi Mohammad, Han Song.* Vila: On pre-training for visual language models // Proceedings of the IEEE/CVF conference on computer vision and pattern recognition. 2024. 26689–26699.

[31] *Lin Weizhe, Byrne Bill.* Retrieval Augmented Visual Question Answering with Outside Knowledge // Proceedings of the 2022 Conference on Empirical Methods in Natural Language Processing. 2022. 11238–11254.

[32] *Lin Weizhe, Chen Jinghong, Mei Jingbiao, Coca Alexandru, Byrne Bill.* Fine-grained late-interaction multi-modal retrieval for retrieval augmented visual question answering // Advances in Neural Information Processing Systems. 36. 2023. 22820–22840.

[33] *Lin Zhihong, Zhang Donghao, Tao Qingyi, Shi Danli, Haffari Gholamreza, Wu Qi, He Mingguang, Ge Zongyuan.* Medical visual question answering: A survey // Artificial Intelligence in Medicine. 2023. 143. 102611.

[34] *Liu Haotian, Li Chunyuan, Li Yuheng, Lee Yong Jae.* Improved baselines with visual instruction tuning // Proceedings of the IEEE/CVF Conference on Computer Vision and Pattern Recognition. 2024. 26296–26306.

[35] *Liu Haotian, Li Chunyuan, Wu Qingyang, Lee Yong Jae.* Visual instruction tuning // Advances in neural information processing systems. 36. 2023. 34892–34916.

[36] *Liu Ye, Li Hui, Garcia-Duran Alberto, Niepert Mathias, Onoro-Rubio Daniel, Rosenblum David S.* MMKG: multi-modal knowledge graphs // The semantic web: 16th international conference, ESWC 2019, portorož, Slovenia, June 2–6, 2019, proceedings 16. 2019. 459–474.

[37] *Luo Haoran, Chen Guanting, Zheng Yandan, Wu Xiaobao, Guo Yikai, Lin Qika, Feng Yu, Kuang Zemin, Song Meina, Zhu Yifan, others .* HyperGraphRAG: Retrieval-Augmented Generation with Hypergraph-Structured Knowledge Representation // arXiv preprint arXiv:2503.21322. 2025.

[38] *Ma Shengjie, Xu Chengjin, Jiang Xuhui, Li Muzhi, Qu Huaren, Yang Cehao, Mao Jiaxin, Guo Jian.* Think-on-Graph 2.0: Deep and Faithful Large Language Model Reasoning with Knowledge-guided Retrieval Augmented Generation // The Thirteenth International Conference on Learning Representations. 2025.

[39] *Marino Kenneth, Rastegari Mohammad, Farhadi Ali, Mottaghi Roozbeh.* Ok-vqa: A visual question answering benchmark requiring external knowledge // Proceedings of the IEEE/CVF conference on computer vision and pattern recognition. 2019. 3195–3204.

[40] *Mensink Thomas, Uijlings Jasper, Castrejon Lluis, Goel Arushi, Cadar Felipe, Zhou Howard, Sha Fei, Araujo André, Ferrari Vittorio.* Encyclopedic vqa: Visual questions about detailed properties of fine-grained categories // Proceedings of the IEEE/CVF International Conference on Computer Vision. 2023. 3113–3124.

[41] *Ni Bo, Liu Zheyuan, Wang Leyao, Lei Yongjia, Zhao Yuying, Cheng Xueqi, Zeng Qingkai, Dong Luna, Xia Yinglong, Kenthapadi Krishnaram, others .* Towards Trustworthy Retrieval Augmented Generation for Large Language Models: A Survey // arXiv preprint arXiv:2502.06872. 2025.

[42] *Ning Liang-bo, Wang Shijie, Fan Wenqi, Li Qing, Xu Xin, Chen Hao, Huang Feiran.* Cheatagent: Attacking llm-empowered recommender systems via llm agent // Proceedings of the 30th ACM SIGKDD Conference on Knowledge Discovery and Data Mining. 2024. 2284–2295.

[43] *Nussbaum Zach, Morris John Xavier, Mulyar Andriy, Duderstadt Brandon.* Nomic Embed: Training a Reproducible Long Context Text Embedder // Transactions on Machine Learning Research. 2025.

[44] *Qi Jingyuan, Xu Zhiyang, Shao Rulin, Chen Yang, Di Jin, Cheng Yu, Wang Qifan, Huang Lifu.* RoRA-VLM: Robust Retrieval-Augmented Vision Language Models // arXiv preprint arXiv:2410.08876. 2024.

[45] *Qu Haohao, Ning Liangbo, An Rui, Fan Wenqi, Derr Tyler, Liu Hui, Xu Xin, Li Qing.* A survey of mamba // arXiv preprint arXiv:2408.01129. 2024.

[46] *Radford Alec, Kim Jong Wook, Hallacy Chris, Ramesh Aditya, Goh Gabriel, Agarwal Sandhini, Sastry Girish, Askell Amanda, Mishkin Pamela, Clark Jack, others .* Learning transferable visual models from natural language supervision // International conference on machine learning. 2021. 8748–8763.

[47] *Ren Shaoqing, He Kaiming, Girshick Ross, Sun Jian.* Faster r-cnn: Towards real-time object detection with region proposal networks // Advances in neural information processing systems. 28. 2015.

[48] *Schwenk Dustin, Khandelwal Apoorv, Clark Christopher, Marino Kenneth, Mottaghi Rozbeh.* A-okvqa: A benchmark for visual question answering using world knowledge // European conference on computer vision. 2022. 146–162.

[49] *Touvron Hugo, Lavril Thibaut, Izacard Gautier, Martinet Xavier, Lachaux Marie-Anne, Lacroix Timothée, Rozière Baptiste, Goyal Naman, Hambro Eric, Azhar Faisal, others .* Llama: Open and efficient foundation language models // arXiv preprint arXiv:2302.13971. 2023.

[50] *Wang P, Bai S, Tan S, Wang S, Fan Z, Bai J, Chen K, Liu X, Wang J, Ge W, others .* Qwen2-vl: Enhancing vision-language model's perception of the world at any resolution, 2024 // URL <https://arxiv.org/abs/2409.12191>. 2024.

[51] *Wang Shijie, Fan Wenqi, Feng Yue, Ma Xinyu, Wang Shuaiqiang, Yin Dawei.* Knowledge Graph Retrieval-Augmented Generation for LLM-based Recommendation // arXiv preprint arXiv:2501.02226. 2025.

[52] *Wu Zhiyu, Chen Xiaokang, Pan Zizheng, Liu Xingchao, Liu Wen, Dai Damai, Gao Huazuo, Ma Yiyang, Wu Chengyue, Wang Bingxuan, others .* Deepseek-vl2: Mixture-of-experts vision-language models for advanced multimodal understanding // arXiv preprint arXiv:2412.10302. 2024.

[53] *Yan Yibin, Xie Weidi.* EchoSight: Advancing Visual-Language Models with Wiki Knowledge // Findings of the Association for Computational Linguistics: EMNLP 2024. 2024. 1538–1551.

[54] *Yuan Xu, Zhou Li, Sun Zenghui, Zhou Zikun, Lan Jingsong.* Instruction-guided multi-granularity segmentation and captioning with large multimodal model // Proceedings of the AAAI Conference on Artificial Intelligence. 2025.

[55] *Zhang Duzhen, Yu Yahan, Dong Jiahua, Li Chenxing, Su Dan, Chu Chenhui, Yu Dong.* MM-LLMs: Recent Advances in MultiModal Large Language Models // Findings of the Association for Computational Linguistics: ACL 2024. 2024. 12401–12430.

[56] *Zhang Tao, Zhang Ziqi, Ma Zongyang, Chen Yuxin, Qi Zhongang, Yuan Chunfeng, Li Bing, Pu Junfu, Zhao Yuxuan, Xie Zehua, others .* mR2AG: Multimodal Retrieval-Reflection-Augmented Generation for Knowledge-Based VQA // arXiv preprint arXiv:2411.15041. 2024.

[57] *Zhao Zihuai, Fan Wenqi, Li Jiatong, Liu Yunqing, Mei Xiaowei, Wang Yiqi, Wen Zhen, Wang Fei, Zhao Xiangyu, Tang Jiliang, others .* Recommender systems in the era of large language models (llms) // IEEE Transactions on Knowledge and Data Engineering. 2024.

[58] *Zhu Jinguo, Wang Weiyun, Chen Zhe, Liu Zhaoyang, Ye Shenglong, Gu Lixin, Tian Hao, Duan Yuchen, Su Weijie, Shao Jie, others .* Internvl3: Exploring advanced training and test-time recipes for open-source multimodal models // arXiv preprint arXiv:2504.10479. 2025.

[59] *Zhu Xiangrong, Xie Yuexiang, Liu Yi, Li Yaliang, Hu Wei.* Knowledge Graph-Guided Retrieval Augmented Generation // arXiv preprint arXiv:2502.06864. 2025.

A. Prompt Design

In our multimodal knowledge graph construction pipeline, we utilize LLMs’ text understanding and generation capabilities to extract textual knowledge graphs automatically by providing appropriate prompts. Since previous work [15, 20] has explored textual KGs extraction, we just follow the prompt template of LightRAG[20].

The core contribution of our mKG-RAG lies in the challenge of merging textual and visual graphs into a multimodal graph. To this end, we employ MLLMs as the vision-text matcher, effectively aligning semantically consistent visual and textual entities/relationships. In this process, we introduce a well-designed vision-text matching prompt to guide the MLLMs, as shown in Figure 5. Moreover, several high-quality examples are provided to MLLMs for In-context Learning. One example is illustrated in Figure 6.

B. Implementation Details

QM-Retriever. In the proposed QM-Retriever, we introduce a Question Converter \mathcal{F}_q to transform interrogative questions into declarative forms, thereby reducing grammatical mismatches with evidence texts. The Question Converter comprises two linear projection layers separated by a ReLU activation function. This transformation is performed in the latent space, where \mathcal{F}_q reformulates the word embeddings of the original questions into declarative representations before passing them to the BERT encoder of the Q-Former.

During training, both the Question Converter \mathcal{F}_q and the Q-Former are jointly optimized, while the Visual Encoder \mathcal{F}_v is kept frozen. The QM-Retriever is trained for 25 epochs on our annotated dataset of 221K query-evidence pairs, using the AdamW optimizer and a CosineLR scheduler with an initial learning rate of 10^{-5} . The training configuration also includes a batch size of 64, a KL divergence coefficient of 2, an input image size of 224×224 , and a maximum token length of 512 for both questions and evidence.

Fine-tuning. Following the experimental setup in ReflectiVA [11], we adopt LLaVA-More [10] as our multimodal answer generator. Since ReflectiVA is specifically optimized for relevant passage filtering and answer generation, we fine-tune our method (mKG-RAG*) accordingly to ensure consistency with this setup. We employ LoRA adapters [24] for parameter-efficient tuning, using a total batch size of 32 and a learning rate of 1.5×10^{-4} . To preserve the model’s performance on established MLLM benchmarks, we augment the fine-tuning dataset with samples from the LLaVA-Instruct-150K dataset [35]. Following the strategy of Wiki-LLaVA [4], we increase the sampling probability of these examples, ensuring they comprise approximately half of each mini-batch.

Vision-Text Matching Prompt

Based on the provided image, visual scene graph, and textual entities and relationships, match visual objects/relations in the image with the provided textual entities/relationships.

Input Format:

Each textual entity are formatted as (“entity”|<entity-name>|<entity-type>|<entity-description>), which contains the following information:

- 1) entity-name: Name of the entity;
- 2) entity-type: Name of the entity type;
- 3) entity-description: Comprehensive description of the entity’s attributes and activities.

Each textual relationship are formatted as (“relation”|<source-entity>|<target-entity>|<relation-description>|<relation-strength>), which contains the following information:

- 1) source-entity: name of the source entity, as defined in the textual entities;
- 2) target-entity: name of the target entity, as defined in the textual entities;
- 3) relation-description: explanation as to why the source entity and the target entity are related to each other;
- 4) relation-strength: a numeric score indicating the strength of the relationship between the source and target entities, ranging from 0 to 10.

The scene graph provides the object and relationship information in the image, which is formatted as:

```
- <object-0>: <object-category>, <object-bbox>  
- <object-1>: <object-category>, <object-bbox>  
...  
- <relation-0>: <object-0> <relation-name> <object-1>  
- <relation-2>: <object-1> <relation-name> <object-3>
```

The <object-bbox> is the bounding box of each object region, represented as (x1, y1, x2, y2) with floating numbers ranging from 0 to 1. These values correspond to the top left x, top left y, bottom right x, and bottom right y.

Matching Steps:

Step 1. Identify the textual entity that is most relevant to the overall image and extract the following information:

- 1) entity-name: the name of the entity that best represents the overall image;
- 2) strength: a numeric score indicating the strength of the match, ranging from 0 to 10.

Format the image matching as (“matching”|<image>|<entity-name>|<strength>)

Step 2. For each object in the scene graph, if the object visually depicts a textual entity identified in the input data, extract the following information:

- 1) object-id: the ID of the object in the scene graph;
- 2) entity-name: the name of the entity it represents;
- 3) strength: a numeric score indicating the strength of the match, ranging from 0 to 10.

Format each object matching as (“matching”|<object-id>|<entity-name>|<strength>)

Step 3. For each relation in the scene graph, if the relation visually represents a textual relationship identified in the input data, extract the following information:

- 1) relation-id: the id of the relation in the scene graph;
- 2) source-entity: the source entity of the relationship it represents;
- 3) target-entity: the target entity of the relationship it represents;
- 4) strength: a numeric score indicating the strength of the match, ranging from 0 to 10.

Format each relation matching as (“matching”|<relation-id>|<source-entity>|<target-entity>|<strength>)

Step 4. For those objects or relations without a corresponding text entity or relationship, please ignore them.

Figure 5: The prompt used to match visual and textual entities/relationships

Vision-Text Matching Example

Textual Entities:

("entity"!MOUNT FUJI!location!Mount Fuji is an active stratovolcano located on Japan's Honshu Island, with a peak elevation of 3,776.24 meters.)
("entity"!HONSHU ISLAND!location!Honshu Island is the largest island of Japan, where Mount Fuji is situated.)
("entity"!CHERRY BLOSSOMS!concept!Cherry blossoms are a symbol of Japan, known for their beauty and cultural significance, often associated with the arrival of spring.)
("entity"!SHINKANSEN!technology!The Shinkansen, also known as the bullet train, is a network of high-speed railway lines in Japan.)

Textual Relationships:

("relationship"!MOUNT FUJI!HONSHU ISLAND!Mount Fuji is located on Honshu Island, making the island its geographical setting.|9)
("relationship"!MOUNT FUJI!CHERRY BLOSSOMS!Both Mount Fuji and cherry blossoms are iconic symbols of Japan, often celebrated together in cultural contexts.|8)
("relationship"!MOUNT FUJI!SHINKANSEN!Mount Fuji and the Shinkansen are both recognized as national symbols of Japan.|7)

Image Description: Mount Fuji and the Shinkansen electric car passing in front of it.

Scene Graph:

- <object-0>: train, (0.06, 0.64, 1.0, 0.77)
- <object-1>: fence, (0.0, 0.8, 0.98, 0.88)
- <object-2>: snow, (0.25, 0.29, 0.67, 0.49)
- <object-3>: mountain, (0.0, 0.3, 1.0, 0.64)
- <relation-0>: <object-0> over <object-1>
- <relation-1>: <object-2> on <object-3>
- <relation-2>: <object-3> behind <object-0>

Output:

("mapping"!<image>!MOUNT FUJI|8)
("mapping"!<object-3>!MOUNT FUJI|9)
("mapping"!<object-0>!SHINKANSEN|7)
("mapping"!<relation-2>!MOUNT FUJI!SHINKANSEN|7)

Figure 6: A high-quality vision-text matching example for In-context Learning